Nanomolding of PEG-Based Hydrogels with Sub-10-nm Resolution**

*Mar Diez, Petra Mela, Venkatash Seshan, Martin Möller, and Marga C. Lensen**

A simple, soft nanolithographic method is used to fabricate sub-10-nm structures on star polyethylene glycol-based hydrogels and perfluoropolyether-based materials. Very small features, for example, gold nanoparticles of size ≈8 nm with an interparticle distance of ≈100 nm, are successfully reproduced from a hard silicon master into both elastomers. Scanning force microscopy is used to investigate the replicas, and the original hexagonal pattern of the nanoparticles is clearly recognized. In addition, both replicas are usable as secondary, soft molds yielding positive copies of the primary, hard master. The results presented here show similar replication capabilities for both elastomers despite the markedly different properties of the precursors. Moreover, the hydrogel material can be easily peeled off from both soft and silicon masters without the need for surface treatment. The procedure allows nanopatterning of a biocompatible material over large areas, which is a useful tool to investigate cellular responses to defined nanotopography.

Keywords:
- elastomers
- fluoropolymers
- hydrogels
- nanolithography
- patterning

1. Introduction

Nowadays the ability to fabricate and manipulate micro- and nanostructures plays an important role in emerging interdisciplinary fields, such as nanobiotechnology. The ever-increasing demand for smaller devices requires improvements of existing manufacturing methodology in many research fields, such as electronics[1–3] and data storage,[4] as well as in nano(bio)technology,[5–7] biosensing,[8] microfluidics,[9] and tissue engineering. Nanotechnology is a field of applied science that involves the development of materials or devices in which at least one of the components has nanoscale dimensions, that is, between 0.1 and 100 nm. Conventional lithographic techniques for micro- and nanofabrication, for example, photolithography or electron-beam lithography (EBL), have been the most viable options for manufacturing tools to reduce the size of, especially, semiconductor and electronic devices.[9–11] However, drawbacks such as resolution limits, fabrication costs, and time make these techniques not optimal when nanometer-sized features are desired over large areas. The challenge is to develop an ideal methodology that combines the possibility of patterning over large areas with high resolution and low-cost production.

In the past few years, progress in the field of microfabrication has encouraged researchers to develop new techniques, such as soft lithography, microcontact printing (μCP), nanoimprint lithography (NIL), nanocontact printing, and scanning probe lithography.[9–11] NIL has pushed nanofabrication to the extent that feature sizes as small as 5 nm and aspect ratios up to 20 have been realized.[12–14] Soft nanolithography has been applied to different materials to produce nanostructures.[15–19] For instance, replication of small, soft (supramolecular) objects, such as viruses, proteins, and micelles, less than 5 nm in size has been demonstrated by the

[*] Dr. M. C. Lensen,[+] M. Diez, Dr. P. Mela, V. Seshan, Prof. M. Möller
DWI e.V. and
Institute of Technical and Macromolecular Chemistry, RWTH Aachen
Pauwelsstrasse 8, 52056 Aachen (Germany)
E-mail: Marga@LensenLab.de

[+] Present address:
Technische Universität Berlin
Institut für Chemie, Sekr. OE 1, Nanostrukturierte Biomaterialien
Franklinstr. 29, 10587 Berlin (Germany)

[**] PEG=polyethylene glycol.

Supporting Information is available on the WWW under http://www.small-journal.com or from the author.

DOI: 10.1002/smll.200901313

small NANO MICRO

DeSimone group.[20] Results by Whitesides et al. show that this technique, which they termed ''replica molding'', can be used to produce features with vertical dimension down to 0.4 nm.[21] However, high-aspect-ratio structures are restricted by pattern deformation processes in soft molds.[22–25] An alternative that combines the benefits of soft lithography and NIL is soft, UV-based NIL (UV-NIL). The simplicity of the technology leads to cost reduction; however, key concerns regarding mold and pattern deformation remain.[25]

Thus, it is clear that not only the imprinting techniques but also the elastomeric materials used in soft nanolithography play a vital role in the fabrication of nanostructures. Elastomeric molds can be sequentially generated, are facile and inexpensive to produce (avoiding the use of clean rooms),[25] and are compatible for applications in biotechnology[9] and electronics, amongst others. A mold material should have ideal properties, such as mechanical integrity yet flexibility, small shrinkage and, if necessary, transparency to UV light. Poly(dimethyl siloxane) (PDMS) has been widely used to fabricate features on the micro- and nanometer scale via soft lithography.[26] PDMS as an elastomer works quite well for most of the soft lithographic processes; however, it has its shortcomings in the limited aspect ratio achievable (due to collapse, pairing, and sagging of relief structures) and poor resistance to organic solvents.[22–26] UV-curable perfluorinated polyether (PFPE) derivatives are exceptionally suitable as alternatives since the cured material is adequately stiff yet flexible enough, so that it does not cause deformation or swelling of the patterned structure.[27–29] These qualities make this fluoropolymer a superior material in comparison to PDMS in the fabrication of soft and inert three-dimensional motifs.[30]

To demonstrate the feasibility of the replica molding technique, various materials, such as polyurethanes, poly(methyl)methacrylates, hard PDMS, and composite elastomers, have been used so far.[15–18,20,31] Here, since we fabricated the replicas for a further application in cell culture, we chose a biomaterial in the last step of nanomolding. Polyethylene glycol (PEG)-based hydrogels are transparent, biocompatible polymers that are known for their suppression of nonspecific cell adhesion and have a high permeability to water and solutes, which is an important criterion for cell culture in biological media.[32] Hydrogels as biomaterials have received a vast amount of interest in recent years for biomedical applications, for example, cell culture, tissue engineering, biosensors, and drug delivery. It has recently been observed that cell adhesion and protein adsorption on (nano)structured PEG substrates increase when compared to smooth PEG substrates.[33,34] Indeed, as described before and also evidenced by our own latest results, the PEG surface topography and elasticity have an influence on the resistance to cell adhesion to biomaterials.[13,35–38] It is a goal in our research to explore cellular responses, such as binding, growth, and migration, on topographic nanopatterned starPEG hydrogels without the need for specific biofunctionalization.

Herein, we present an easy and cheap bench-top method to pattern PEG-based hydrogels with ultrafine structures over large areas, while avoiding the use of expensive masters, clean-room conditions, or the need for mold release agents. The patterning of these hydrogels with spatially controlled nanotopography provides suitable substrates for the investigation of cell response to nanostructures.

2. Results and Discussion

The masters employed in this study consist of ultrafine structures: arrays of gold nanoparticles, which are created on silicon wafers via block-copolymer-micelle nanolithography.[39–42] A clear advantage of this technique is the possibility of patterning large areas; in principle wafer-scale patterning is possible. Without additional patterning procedures the gold-loaded block-copolymer micelles organize themselves into a close-packed arrangement, which eventually results in hexagonal arrays of nanometer-sized gold particles (in our case ranging from 1 to 15 nm in size depending on the amount of salt loaded in the core and the poly(2-vinyl pyridine) units). The interparticle distance depends on the micelle diameter and can be chosen between 20 and 200 nm. In this study, we used the same block copolymer and two concentrations of gold salt, which led to gold nanoparticles 7 and 9 nm in size, respectively, and with an average interparticle spacing of 100 nm. The masters were studied by atomic force microscopy (AFM). The hexagonal pattern of the gold nanoparticles on the surface of the silicon can be easily recognized (Figure 1a and Figure 3a),

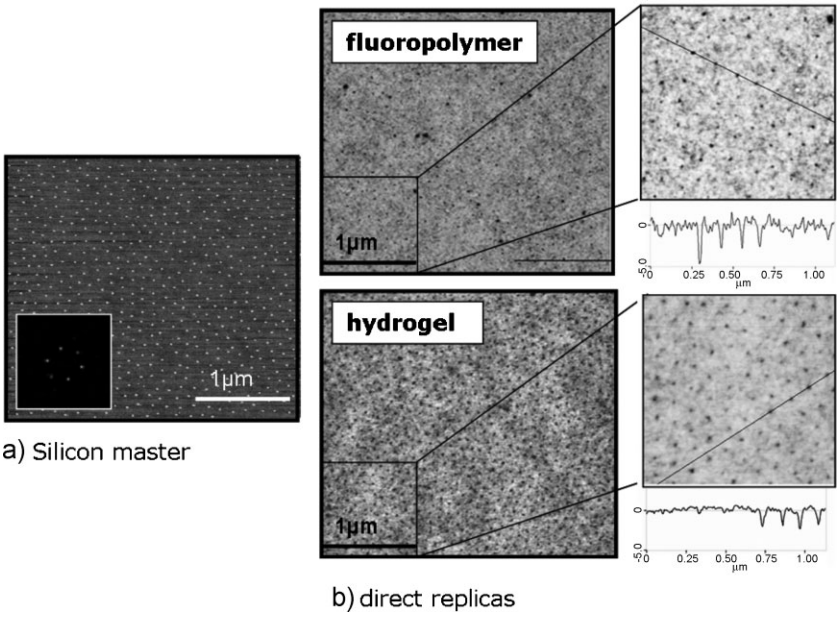

Figure 1. AFM images ($3 \times 3\ \mu m^2$) with height scale 5 nm of a) the nanostructured silicon master and b) direct replicas from (a); fluoropolymer replica (top) and hydrogel replica (bottom). The images on the right are $1 \times 1\ \mu m^2$ in size and AFM line scans are depicted.

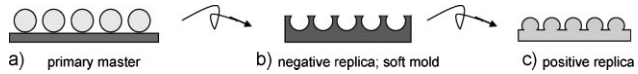

Figure 2. Secondary mold method. a) Primary mold: silicon master decorated with gold nanoparticles. b) Secondary mold: elastomeric mold made of fluoropolymer or hydrogel. c) Positive replica of the primary master of hydrogel or fluoropolymer.

and Fourier transformation (FT) on the height image (inset in Figure 1a) confirmed this arrangement.

The photocurable prepolymer mixtures (PFPE mix and starPEG mix) were drop-cast onto the structured masters and cured by UV light leading to transparent, stand-alone elastomeric films. As expected based on previous results,[20,40] the fluoropolymer successfully replicates sub-10-nm features from the silicon surfaces. Figure 1b (top) shows AFM images of the nanoindents on its surface. This material allows easy detachment from the original hard mold with no residual adhesion observed.

Surprisingly, the hydrogel can also be structured and easily detached from the same hard master with no greater effort than was experienced in the case of the fluoropolymer, despite the fact that surface treatment is often reported to be necessary to facilitate the release of organic materials from hard masters.[43] Figure 1b (bottom) shows the regular, hexagonal distribution of nanoindents on the surface of the hydrogel obtained directly from the silicon master.

To obtain a positive replica of the primary masters, a second mold methodology was employed (Figure 2). The fluoropolymer was used as a mold to replicate the hydrogel and, as a novelty, vice versa. The soft molds are durable in many replication cycles with no noticeable degradation or deformation of the structures. As for the positive replicas, on both materials the well-defined, hexagonal pattern of nanoprotrusions is recognized and has good resemblance to the primary master (Figure 3).

Figure 3b and c show AFM images of the negative replicas used as molds and of the corresponding positive replicas, respectively. It was already known that the fluoropolymer is able to replicate ultrafine structures and could be used as a soft secondary mold (Figure 3, route 1), but now we have discovered that the hydrogel also has this versatile ability. Strikingly, the nanopatterned hydrogel can be used as a secondary, soft mold in a similar way to the fluoropolymer (Figure 3, route 2). The hexagonal order of the protrusions was verified by FT (images not shown).

Before analyzing the replicas in further detail, that is, comparing the height of the protrusions with the original nanoparticles (see below), it should be noted that the quality of the hydrogel replicas seems even better than that of the fluoropolymer replicas. The apparently clearer images in the case of the hydrogel could be due to differences in the inherent roughness of the materials. The higher surface energy of the hydrogel might result in a flattening of the surface, and thus the ultrafine structures appear more evident than those masked by the roughness of the polymer; a case in point is the fluoropolymer. The roughness of the fluoropolymer and hydrogel surfaces (root mean square (rms) (0.55 ± 0.1) and (0.42 ± 0.04) nm, respectively) is not very different from that of the silicon wafer used as a master (rms (0.43 ± 0.3) nm), but is smoother in the case of the hydrogel.

To evaluate the dimensions of the structures, AFM was the method of choice. Table 1 shows an averaged value of the dimensions of the structures. In the case of the indentations, it was not possible to accurately evaluate the depth, which can be understood when taking the size of the AFM tip and the corresponding deconvolution of its shape into consideration. However, when molding from the negative replicas the size of the nanoprotrusions is close to that of the original nanoparticles, notably in the case of the fluoropolymer. It seems that all nanofeatures on the hydrogel appear smaller than those on the fluoropolymer replicas. There are several reasons that could

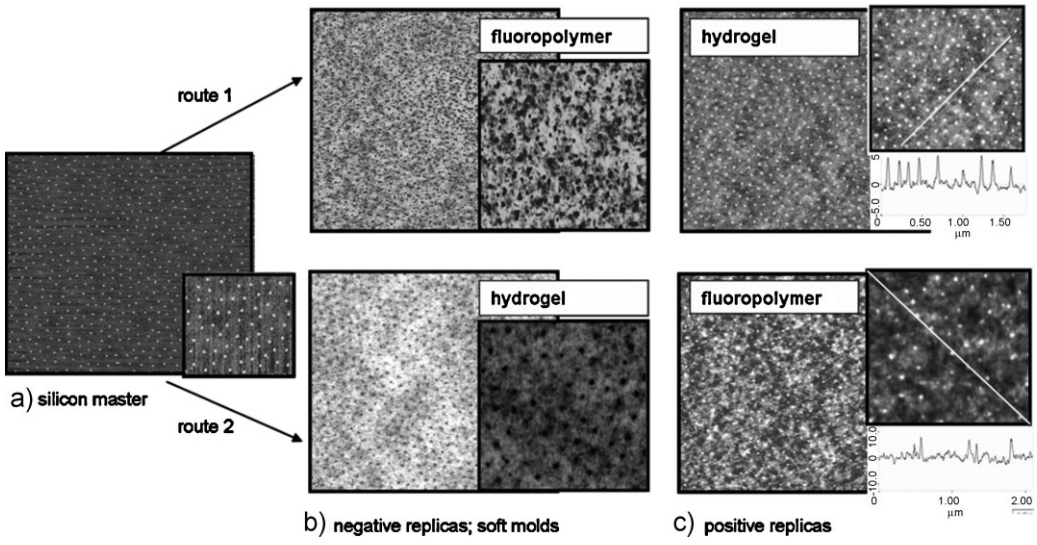

Figure 3. AFM images ($3 \times 3\ \mu m^2$) with height scale 5 nm of a) the nanostructured silicon master and b) direct replicas from the silicon master shown in (a): fluoropolymer replica (top) and hydrogel replica (bottom). c) Replicas from soft molds shown in (b): hydrogel replica from fluoropolymer and fluoropolymer replica from hydrogel mold (height scale 10 nm) and the corresponding AFM line scans.

NANO MICRO small

Table 1. Feature sizes on the silicon master and on the elastomeric replicas as observed by AFM. Negative signs indicate the depth of the indents and positive numbers indicate the height of the protrusions.

Master [nm]		Fluoropolymer replica [nm]	Hydrogel replica [nm]
Silicon master with nanoparticles	9.0 ± 1.0	-5.0 ± 0.6	-2.3 ± 0.3
Fluoropolymer mold	-5.0 ± 0.6	6.9 ± 0.5	4.6 ± 0.1
Hydrogel mold	-2.3 ± 0.3	7.5 ± 0.7	4.4 ± 0.5

account for this observation. Here we consider and discuss three aspects that are related to the nature of the materials: the stiffness and wettability of the gels and the viscosity of the precursors.

It has been reported how the surface topography at the nanoscale for materials prepared by NIL, embossing, and replica molding strongly depends on the elasticity and surface tension of the material.[24,44–46] As discussed before, a higher surface energy of the hydrogel might result in the smoothening of the structures; consequently, the features appear smaller than they should be. It has been described how soft materials lose mechanical integrity and hence the pattern deforms.[22–24] Therefore, the soft nature of the hydrogel may lead to mold deformation effects such as sagging that reduce the size of the structures. On top of that, hydrogels may swell and soften under the influence of relative humidity, thus resulting in even shallower protrusions. In the case of the stiffer fluoropolymer, the patterned structures are not expected to experience such deformations, and the height of the protrusions resembles more closely the height of the gold nanoparticles on the original silicon master. To verify this reasoning, the stiffness of the hydrogel was modified by varying the crosslinking density. Hydrogels with stiffness differing by one order of magnitude were prepared, that is, having a modulus of 0.2 MPa (softer), 1 MPa (standard in this study), or 3 MPa (stiffer). The elasticity of the latter is comparable with that of the fluoropolymer (≈4 MPa). Both softer and stiffer hydrogel replicas were evaluated and the values observed were ≈4.5 nm in both cases (images not shown), analogous to the size found for the gel with intermediate stiffness. The similarities in height for the hydrogels with different mechanical properties seem to discard softness as a cause of the differences in the size of the features patterned on the hydrogel when compared to the fluoropolymer material.

The next aspect considered is the wettability of the elastomeric molds. The lower wettability of the hydrophobic fluoropolymer surface may not allow the viscous hydrogel precursor to completely fill the indents of the mold (Figure 4). On the other hand, the higher surface energy, and hence favorable wetting, of the hydrophilic hydrogel allows the liquid, hydrophobic PFPE precursor to spread and follow the contour of the mold. To investigate the poor wettability of the fluoropolymer mold as the cause of the different resolution of the structures, both the hydrogel and fluoropolymer molds were replicated by their own liquid precursor mixtures, starPEG mix and PFPE mix, respectively. The hydrogel replica again showed small protrusions of size (4.4 ± 0.5) nm and the fluoropolymer again displayed larger protrusions of size (6.9 ± 0.5) nm, despite the low surface energy of the fluoropolymer mold. A more favorable wetting on the hydrogel surface is apparently not sufficient explanation of the different heights in hydrogel and fluoropolymer either.

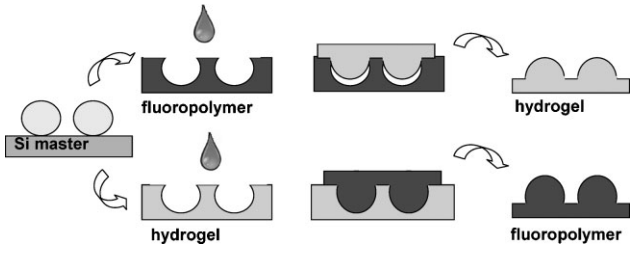

Figure 4. Secondary mold approach for hydrogel (light gray) and fluoropolymer (dark gray).

Regardless of the mold material, the protrusions on the hydrogel are always smaller than those on the fluoropolymer, hence not only the nature of the cured material but also the properties of the precursor mixture seem to influence the resulting structures. A last aspect that is considered is the viscosity of the precursor mixtures, which might also influence the fidelity of the replicas.[19] The liquid PFPE mix has a low viscosity (≈0.48 Pa s) in addition to its lubricating properties,[28] which ensures the accurate filling of the mold. The more viscous starPEG mix (≈2.7 Pa s), on the other hand, may not be able to spread properly on the elastomeric surfaces, neither in the fluoropolymer nor in the hydrogel mold due to a too high viscosity, which results in shallower features on the replicas. We performed two sets of experiments to verify whether the viscosity plays an important role. First, we let the precursor mix longer (several days) on the mold before curing. Second, we diluted the starPEG mix with a solvent (acetone) to decrease its viscosity. However, in neither of the two cases did we find larger protrusions on the replicas. At this stage we must conclude that probably the combination of surface energy and softness led to the observed smaller heights of the protrusions. Nevertheless, since the material is soft, AFM might not be able to give adequate numbers in the first place.

The purpose of this study was to demonstrate that sub-10-nm features could be replicated on the surface of a biocompatible hydrogel with high reproducibility. Initially, replica molding was carried out using a soft, fluoropolymer mold to ensure excellent mold release, first from the primary silicon master and second from the hydrogel replica. Surprisingly, we found that the nanomolding of the hydrogel could also be carried out directly from the silicon master, without treating the master with a release agent.

3. Conclusions

Sub-10-nm features have been patterned on two polymeric materials with very different properties: a very hydrophobic fluoropolymer and a very hydrophilic hydrogel. The fluorinated

material showed its expected capability of high fidelity replication. Here, we have shown how starPEG-based hydrogels can be effectively patterned from either a hard (silicon) master or a soft mold, without the need for surface treatment.

This facile method permits high-resolution, high-fidelity patterning over large areas on the surface of a biocompatible material, and avoids extra steps for surface treatment or clean-room conditions. Both the simplicity and cost efficiency of this procedure underline its potential use in nanomanufacturing. Due to the nontoxic nature, biocompatibility, and patterning versatility of these materials, we expect them to have a significant role in biological applications as well as in nanotechnology development.

4. Experimental Section

Experimental procedures and AFM images of the micelles on the silicon wafer and the gold nanoparticles on the silicon wafer before and after replication are available on the Supporting Information.

Acknowledgements

The authors would like to thank the Alexander von Humboldt Foundation and the German Federal Ministry for Education and Research (BMBF) for funding in the form of a Sofja Kovalevskaja Award (M.C.L.).

[1] C. C. Cedeno, J. Seekamp, A. P. Kam, T. Hoffmann, S. Zankovych, C. M. Sotomayor Torres, C. Menozzi, M. Cavallini, M. Murgia, G. Ruani, F. Biscarini, M. Behl, R. Zentel, J. Ahopelto, *Microelectron. Eng.* **2002**, *61–2*, 25–31.
[2] X. Cheng, Y. Hong, J. Kanicki, J. Guo, *J. Vac. Sci. Technol. B* **2002**, *20*, 2877–2880.
[3] M. C. McAlpine, R. S. Friedman, C. M. Lieber, *Nano Lett.* **2003**, *3*, 443–445.
[4] G. M. McClelland, M. W. Hart, C. T. Rettner, M. E. Best, K. R. Carter, B. D. Terris, *Appl. Phys. Lett.* **2002**, *81*, 1483–1485.
[5] D. Falconnet, D. Pasqui, S. Park, R. Eckert, H. Schift, J. Gobrecht, R. Barbucci, M. Textor, *Nano Lett.* **2004**, *4*, 1909–1914.
[6] J. D. Hoff, L. J. Cheng, E. Meyhöfer, L. J. Guo, A. J. Hunt, *Nano Lett.* **2004**, *4*, 853–857.
[7] W. Hu, E. K. F. Yim, R. M. Reano, K. W. Leong, S. W. Pang, *J. Vac. Sci. Technol. B* **2005**, *23*, 2984–2989.
[8] K. Kuwabara, *Microelectron. Eng.* **2004**, *73–74*, 752–756.
[9] G. M. Whitesides, E. Ostuni, S. Takayama, X. Jiang, D. E. Ingberet, *Annu. Rev. Biomed. Eng.* **2001**, *3*, 335–373.
[10] B. D. Gates, Q. Xu, M. Stewart, R. Ryan, C. G. Willson, G. M. Whitesides, *Chem. Rev.* **2005**, *105*, 1171–1196.
[11] A. del Campo, E. Arzt, *Chem. Rev.* **2008**, *108*, 911–945.
[12] K. Ansari, J. A. van Kan, A. A. Bettiol, F. Watt, *Appl. Phys. Lett.* **2004**, *85*, 476–478.
[13] M. D. Austin, H. Ge, W. Wu, M. Li, Z. Yu, D. Wasseman, S. A. Lyon, Y. Chou, *Appl. Phys. Lett.* **2004**, *84*, 5299–5301.
[14] S. Y. Chou, P. R. Krauss, P. J. Renstrom, *J. Vac. Sci. Technol. B* **1997**, *15*, 2897–2904.
[15] S. J. Choi, P. J. Yoo, S. J. Baek, T. W. Kim, H. H. Lee, *J. Am. Chem. Soc.* **2004**, *126*, 7744–7745.
[16] B. D. Gates, G. M. Whitesides, *J. Am. Chem. Soc.* **2003**, *125*, 14986–14987.
[17] N. Y. Lee, J. R. Lim, M. J. Lee, J. B. Kim, S. J. Jo, H. K. Baik, Y. S. Kim, *Langmuir*, **2006**, *22*, 9018–9022.
[18] Y. N. Xia, J. J. McClelland, R. Gupta, D. Qin, X. M. Zhao, L. L. Sohn, R. J. Celota, G. M. Whitesides, *Adv. Mater.* **1997**, *9*, 147–149.
[19] N. Koo, U. Plachetka, M. Otto, J. Bolten, J. Jeong, E. Lee, H. Kurz, *Nanotechnology* **2008**, *19*, 225304–225307.
[20] B. W. Maynor, I. LaRue, Z. Hu, J. P. Rolland, P. Pandyo, Q. Fu, J. Liu, R. J. Spontak, S. S. Sheiko, R. J. Samulski, E. T. Samulski, J. M. DeSimone, *Small* **2007**, *3*, 845–849.
[21] Q. B. Xu, B. T. Mayers, M. Lahav, D. V. Vezenov, G. M. Whitesides, *J. Am. Chem. Soc.* **2005**, *127*, 854–855.
[22] E. Delamarche, H. Schmid, B. Michel, H. Biebuyck, *Adv. Mater.* **1997**, *9*, 741–746.
[23] Y. G. Y. Huang, W. Zhou, K. J. Hsia, E. Menard, J. Park, J. A. Rogers, A. G. Alleyne, *Langmuir* **2005**, *21*, 8058–8068.
[24] C. Y. Hui, A. Jagota, Y. Y. Lin, E. J. Kramer, *Langmuir* **2002**, *18*, 1394–1407.
[25] Y. N. Xia, G. M. Whitesides, *Annu. Rev. Mater. Sci.* **1998**, *37*, 551–575.
[26] W. M. Choi, O. O. Park, *Microelectron. Eng.* **2004**, *73–74*, 178–183.
[27] J. P. Rolland, E. C. Hagberg, G. M. Denison, K. R. Carter, J. M. DeSimone, *Angew. Chem.* **2004**, *116*, 5920–5923. *Angew. Chem. Int. Ed.* **2004**, *43*, 5796–5799.
[28] J. P. Rolland, M. Van Dam, D. A. Schorzman, S. R. Quake, J. M. DeSimone, *J. Am. Chem. Soc.* **2004**, *126*, 2322–2323.
[29] T. T. Truong, R. S. Lin, S. Jeon, H. H. Lee, J. Maria, A. Gaur, F. Hua, I. Meinel, J. A. Rogers, *Langmuir* **2007**, *23*, 2898–2905.
[30] J. P. Rolland, B. W. Maynor, L. E. Euliss, A. E. Exner, G. M. Denison, J. M. DeSimone, *J. Am. Chem. Soc.* **2005**, *127*, 10096–10100.
[31] Z. H. Nie, E. Kumacheva, *Nat. Mater.* **2008**, *7*, 277–290.
[32] J. H. Harris, *Poly(Ethylene Glycol) Chemistry: Biotechnical and Biomedical Applications*. Plenum Press, New York **1993**.
[33] P. Kim, D. H. Kim, B. Kim, S. K. Choi, S. H. Lee, A. Khademhosseini, R. Langer, K. Y. Suh, *Nanotechnology* **2005**, *16*, 2420–2426.
[34] M. C. Lensen, V. A. Schulte, J. Salber, M. Díez, F. Menges, M. Möller, *Pure Appl. Chem.* **2008**, *80*, 2479–2487.
[35] R. J. Pelham, Y. L. Wang, *Proc. Natl. Acad. Sci. USA* **1998**, *95*, 12070–12070.
[36] T. Yeung, P. C. Georges, L. A. Flanagan, B. Marg, M. Ortiz, M. Funaki, N. Zahir, W. Y. Ming, V. Weaver, P. A. Janmey, *Cell Motil. Cytoskeleton* **2005**, *60*, 24–34.
[37] D. H. Kim, P. Kim, I. Song, J. M. Cha, S. H. Lee, B. Kim, K. Y. Suh, *Langmuir* **2006**, *22*, 5419–5426.
[38] Y. Lu, J. Sun, J. Shen, *Langmuir* **2008**, *24*, 8050–8055.
[39] J. P. Spatz, S. Mössmer, C. Hartmann, M. Möller, T. Herzog, M. Krieger, H. G. Boyen, P. Ziemann, B. Kabius, *Langmuir* **2000**, *16*, 407–415.
[40] M. C. Lensen, P. Mela, A. Mourran, J. Groll, J. Heuts, H. T. Rong, M. Möller, *Langmuir* **2007**, *23*, 7841–7846.
[41] R. Glass, M. Arnold, E. A. Cavalcanti-Adam, J. Blummel, C. Haferkemper, C. Dodd, J. P. Spatz, *New J. Phys.* **2004**, *6*, 101.
[42] R. Glass, M. Möller, J. P. Spatz, *Nanotechnology* **2003**, *14*, 1153–1160.
[43] H. Schift, S. Park, B. Y. Jung, C. G. Choi, C. S. Kee, S. P. Han, K. B. Yoon, J. Gobrecht, *Nanotechnology* **2005**, *16*, S261–S265.
[44] O. D. Gordan, B. N. J. Persson, C. M. Cesa, D. Mayer, B. Hoffmann, S. Dieluweit, R. Merkel, *Langmuir* **2008**, *24*, 6636–6639.
[45] H. D. Rowland, A. C. Sun, P. R. Schunk, W. P. King, *J. Micromech. Microeng.* **2005**, *15*, 414–2425.
[46] Y. N. Xia, D. Qin, Y. D. Yin, *Curr. Opin. Colloid Interface Sci.* **2001**, *6*, 54–64.

Received: July 22, 2009
Published online: September 28, 2009

